 doi:10.20944/preprints202010.0017.v1

Article

Transition from Electromechanical Dynamics to Quasi-Electromechanical Dynamics Caused by Participation of Full Converter-based Wind Power Generation

Jianqiang Luo [1], and Siqi Bu [1]*

[1] Department of Electrical Engineering, The Hong Kong Polytechnic University, Hong Kong.
jq.luo@connect.polyu.hk
* Correspondence: siqi.bu@polyu.edu.hk

Abstract: Previous studies generally reckon that the full converter-base wind power generation (FCWG) is a 'decoupled' power source from the grid, which hardly participates in electromechanical oscillations. However, it is found recently that strong interaction could be induced which might incur severe resonance incidents in electromechanical dynamic timescale. In this paper, the participation of FCWG in electromechanical dynamics is extensively investigated, and particularly, an unusual transition of electromechanical oscillation mode (EOM) is uncovered for the first time. The detailed mathematical models of open-loop and closed-loop power systems are firstly established, and modal analysis is employed to quantify the FCWG participation in electromechanical dynamics, with two new mode identification criteria, i.e., FCWG dynamics correlation ratio (FDCR) and quasi-electromechanical loop correlation ratio (QELCR). On this basis, the impact of different wind penetration levels and controller parameter settings on the participation of FCWG is investigated. It is revealed that if an FOM has a similar oscillation frequency to the system EOMs, there is a high possibility to induce strong interactions between FCWG dynamics and system electromechanical dynamics of the external power systems. In this circumstance, an interesting phenomenon may occur that an EOM may be dominated by FCWG dynamics, and hence is transformed into a quasi-EOM, which actively involves the participation of FCWG quasi-electromechanical state variables.

Keywords: Electromechanical dynamics; FCWG dynamics; strong interaction; electromechanical loop correlation ratio (ELCR); FCWG dynamic correlation ratio (FDCR); quasi- electromechanical loop correlation ratio (QELCR)

1. Introduction

The high penetration of renewables and power electronic domination are two important aspects in the future power system [1, 2]. Converter integrated generations (CIGs) such as wind power and photovoltaic (PV) generation have been increasingly integrated into the power system at an incredible scale and speed and play a pivotal role in rendering the power system more sustainable [3-5]. As one of promising CIGs, full converter-based wind power generation (FCWG, e.g. permanent magnet synchronous generator (PMSG)), in which two full scale converters are employed to transfer wind power to the power system, has become prevalent in the wind market due to its concise physical structure and mature control techniques [6-9]. The ever-increasing share of wind generation and its replacement of conventional synchronous generator (SGs) involve profound challenges on the electromechanical dynamics and potential threat on the oscillatory stability of the power system [10-13]. Unlike conventional rotational power source, the integration of FCWG may introduce complex interactions with the electromechanical dynamics, which is well worth investigating, whereas it has not been thoroughly studied.

 doi:10.20944/preprints202010.0017.v1

Currently, many efforts have been endeavored to how to utilize wind generation and employ various additional controllers to mitigate electromechanical oscillations. Despite the inertia-less characteristic under maximum power point tracking (MPPT) control strategy, by emulating an inertia response, double fed inductor generator (DFIG) is capable in damping electromechanical oscillations [14]. Both drivetrain torsional oscillations of DFIG and electromechanical oscillations are further examined, and alternative dampers are designed to suppress these oscillations [15]. The potential of imposing inter-area oscillation damping control with wind power plants is studied in [16]. The effect of spatial correlation between wind speed of geographically close wind farms on the damping of electromechanical oscillations is examined in [17]. With the aid of wide area measurement system, a wide area damping controller is designed for DIFGs to alleviate electromechanical oscillations [18]. A second-order slide-mode based damping controller is proposed in [19] and [20] as a resort for inter-area oscillation mitigation. A reduced-order model based optimal oscillation damping controller is also designed in [21]. Residue-based evaluation method is implemented to provide additional control design for the power oscillations [22]. In addition, modulation and coordination resorts such as active power modulation and reactive power modulation [23] and DC-link control [24] are also proposed to damp inter-area oscillations with wind generation.

Apart from mitigating electromechanical oscillations with wind generation, the dynamic interactions between wind generation and the electromechanical dynamics have also drawn attention and defined as a converter-driven stability problem [3]. Model validation and reduction techniques for different types of wind power induction generator (i.e. fixed-speed induction generator (FSIG), DFIG) are discussed in terms of oscillation stability issues [25-27]. The dynamic interaction between wind generation and the electromechanical modes of the nearby synchronous generators (SGs) poses threat on the small signal stability with high penetration levels of wind power, which is verified with modal analysis techniques [28]. A electric torque analysis method is proposed in [29] to quantify the impact of wind generation integration on electromechanical oscillations. A novel modal superposition theory is proposed in [30] to classify the interaction categories between wind generation and the external power system. The impact of power electronic integrated wind generation considering increasing wind penetration and load conditions on the inter-area oscillation is investigated in [31].

Although these works above have validated the impact of wind generation on electromechanical dynamics and provided satisfactory solutions to tackle the electromechanical oscillations with various control resorts, the systematic modelling to deepen the understanding of FCWG participation in electromechanical dynamics is still worth further exploring. Especially, an interesting phenomenon is discovered that, under some circumstance, the electromechanical oscillation mode (EOM) may be dominated by the FCWG dynamics and become a quasi-EOM, which has not been studied before. Therefore, the main contributions of this paper are summarized as: 1) a linearized open-loop and closed-loop power system model tailored for FCWG dynamics impact investigation is established; 2) together with the electromechanical loop correlation ratio (ELCR), an FCWG dynamics correlation ratio (FDCR) and quasi-ELCR (QELCR) are proposed to quantify the participation of FCWG in electromechanical dynamics; 3) extensive case studies considering comprehensive wind penetration levels are thoroughly examined to uncover the unusual transition in electromechanical dynamics; and 4) useful findings and suggestions on how FCWG dynamics transform both local and inter-area mode are provided based on modal analysis and time domain

Preprints (www.preprints.org) | NOT PEER-REVIEWED | Posted: 1 October 2020 doi:10.20944/preprints202010.0017.v1

simulations.

The remaining of this paper is organized as follows. Section 2 presents a typical configuration of FCWG. Section 3 proposes a method to investigate the participation of FCWG by constructing the open-loop linearized power system model and the closed-loop linearized power system model. In Section 4, the participation of FCWG is meticulously examined in a two-area test system, and important findings on the impact of the electromechanical dynamics are concluded. Main findings are summarized in Section 5 while conclusions are stressed in Section 6.

2. Configuration of FCWG

The typical topology of an FCWG (e.g. permanent magnetic synchronous generator (PMSG)) connected to the multimachine power system is demonstrated in **Figure 1**.

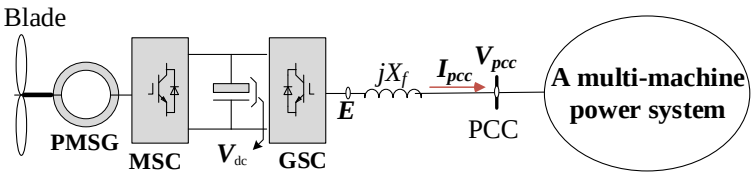

Figure 1. Physical configuration of an FCWG connected to a multi-machine power system.

The FCWG consists of three parts: 1) The PMSG, the machine side converter (MSC) and the associated control system (as demonstrated in **Figure 2**); 2) The DC-link, the grid side converter (GSC) and the associated control system (as shown in **Figure 3**); and 3) The synchronous reference frame phase-locked loop (SRF-PLL) (as presented in **Figure 4**), which is used to synchronize FCWG with the external power system.

The electromechanical dynamics stems from the inertia sources of power systems. Regarding the large mass of physical rotors, SGs are the main inertia sources of the conventional power system, which actuate as a buffer under unintended disturbance contingencies and bolster the oscillatory stability. Owing to the AC-DC-AC configuration, the rotor inertia of wind turbine is decoupled from the multimachine power system, and hence FCWG is normally regarded as a low-inertia source. Such low-inertia characteristic is significantly distinguished from the conventional power sources like SGs. Therefore, the integration of FCWG is usually recognized to be inertia-less which may not participate in electromechanical dynamics like SGs. Its impact on electromechanical dynamics is not taken into account meticulously.

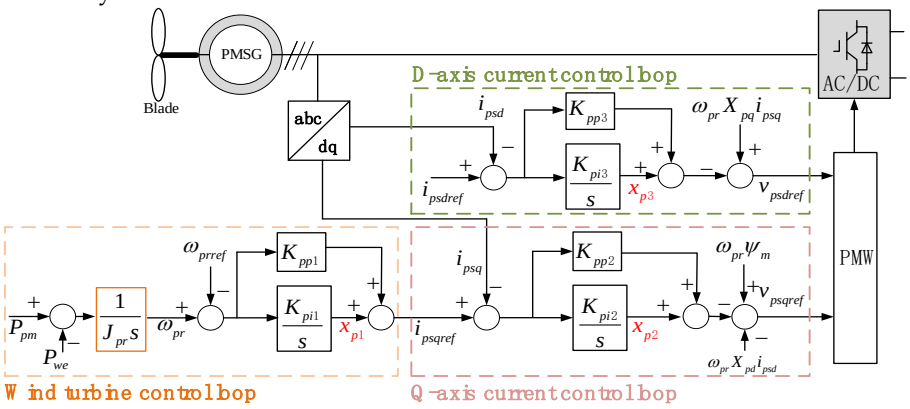

Figure 2. The control configuration of machine side converter (MSC).

Preprints (www.preprints.org) | NOT PEER-REVIEWED | Posted: 1 October 2020 doi:10.20944/preprints202010.0017.v1

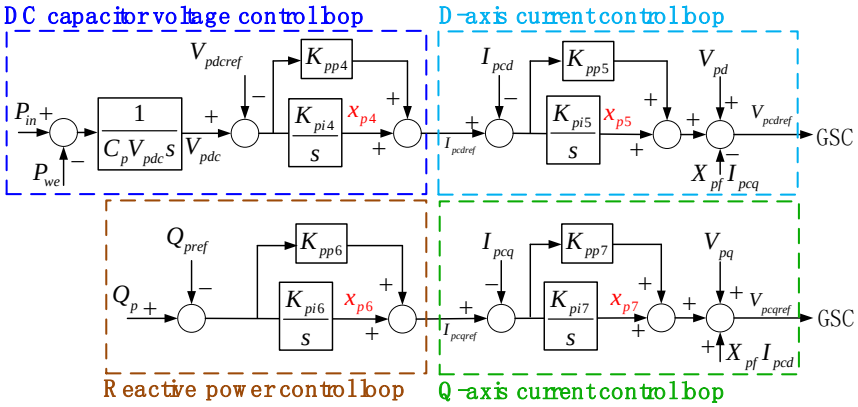

Figure 3. The control configuration of grid side converter (GSC).

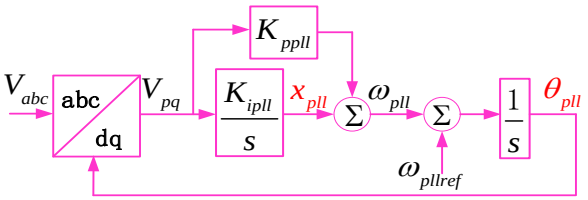

Figure 4. Block diagram of SRF-PLL.

3. Modal Analysis on Electromechanical Dynamics and FCWG Dynamics

Comprehensive modal analyses on the electromechanical oscillation modes (EOMs) are carried out to essentially reveal the participation mechanism of FCWG in electromechanical dynamics. To elaborate the participation of FCWG, the power system excludes the FCWG dynamics is denoted as the open-loop power system, while the entire system is the closed-loop power system. By comparing the EOMs of the open-loop and closed-loop power system, the impact of FCWG is quantified.

3.1. State-space model of FCWG

The state-space model of FCWG is expressed as

$$\begin{cases} \dfrac{d}{dt}\Delta X_W = A_W \Delta X_W + B_W \Delta V_W \\ \Delta I_W = C_W \Delta X_W \end{cases} \tag{1}$$

where ΔX_W denotes all the state variables of FCWG (as illustrated in **Figure 2~Figure 4**); A_W, B_W, C_W are the state-space matrices after integrating all the linearized differential equations.

3.2. Open-loop Power System

By regarding the FCWG as a constant power source, the dynamics of FCWG is excluded in the power system. The state-space model of the ith SG in the power system can be expressed as

$$\begin{cases} \dfrac{d}{dt}\Delta X_{gi} = A_{gi} \Delta X_{gi} + B_{gi} \Delta V_{gi} \\ \Delta I_{gi} = C_{gi} \Delta X_{gi} + D_{gi} \Delta V_{gi} \end{cases} \tag{2}$$

where ΔX_{gi} is the state variables of SG i; A_{gi}, B_{gi}, C_{gi}, D_{gi} are the state-space matrices; ΔV_{gi} and ΔI_{gi} are voltage variation and current variation at the connecting bus of SG i respectively.

The equation of transmission network is express as

$$\begin{bmatrix} \Delta I_g \\ 0 \end{bmatrix} = \begin{bmatrix} Y_{gg} & Y_{gN} \\ Y_{Ng} & Y_{NN} \end{bmatrix} \begin{bmatrix} \Delta V_g \\ \Delta V_N \end{bmatrix} = Y_{open} \begin{bmatrix} \Delta V_g \\ \Delta V_N \end{bmatrix} \tag{3}$$

Preprints (www.preprints.org) | NOT PEER-REVIEWED | Posted: 1 October 2020 doi:10.20944/preprints202010.0017.v1

where ΔI_g denotes the current variation at generator buses; ΔV_g and ΔV_N are the voltage variation at generator buses and other buses; Y_{open} is the open-loop admittance matrix of transmission network in which the FCWG is reckoned as a constant power source and modeled as a constant impedance. Assume that the total number of SGs is M, then

$$\begin{aligned}
\Delta I_g &= \begin{bmatrix} \Delta I_{g1} & \Delta I_{g2} & \cdots & \Delta I_{gM} \end{bmatrix}^T \\
\Delta V_g &= \begin{bmatrix} \Delta V_{g1} & \Delta V_{g2} & \cdots & \Delta V_{gM} \end{bmatrix}^T \\
\Delta X_g &= \begin{bmatrix} \Delta X_{g1} & \Delta X_{g2} & \cdots & \Delta X_{gM} \end{bmatrix}^T \\
A_g &= \mathrm{diag}\begin{bmatrix} \Delta A_{g1} & \Delta A_{g2} & \cdots & \Delta A_{gM} \end{bmatrix}^T \\
B_g &= \mathrm{diag}\begin{bmatrix} \Delta B_{g1} & \Delta B_{g2} & \cdots & \Delta B_{gM} \end{bmatrix}^T \\
C_g &= \mathrm{diag}\begin{bmatrix} \Delta C_{g1} & \Delta C_{g2} & \cdots & \Delta C_{gM} \end{bmatrix}^T \\
D_g &= \mathrm{diag}\begin{bmatrix} \Delta D_{g1} & \Delta D_{g2} & \cdots & \Delta D_{gM} \end{bmatrix}^T
\end{aligned} \tag{4}$$

where diag[] represents the diagonal matrix. By integrating all the SGs together, the state-space model is expressed as

$$\begin{cases} \dfrac{d}{dt}\Delta X_g = A_g \Delta X_g + B_g \Delta V_g \\ \Delta I_g = C_g \Delta X_g + D_g \Delta V_g \end{cases} \tag{5}$$

From (3), the relationship between ΔI_g and ΔV_g can be expressed as

$$\Delta I_g = (Y_{gg} - \frac{Y_{gN} Y_{Ng}}{Y_{NN}})\Delta V_g \tag{6}$$

Combine (5) and (6), the state-space model of the open-loop power system is derived as

$$\frac{d}{dt}\Delta X_g = [A_g + \frac{B_g C_g}{Y_{gg} - \dfrac{Y_{gN} Y_{Ng}}{Y_{NN}} - D_g}]\Delta X_g = A_{open}\Delta X_g \tag{7}$$

where A_{open} is characteristic matrix of the open-loop power system.

3.3. Closed-loop Power System

In this subsection, the dynamics of FCWG is considered by injective a current variation ΔI_W into the external power system. Accordingly, the network equation in (3) should be modified as below

$$\begin{bmatrix} \Delta I_g \\ \Delta I_W \\ 0 \end{bmatrix} = \begin{bmatrix} Y_{gg} & Y_{gW} & Y_{gN} \\ Y_{Wg} & Y_{WW} & Y_{WN} \\ Y_{Ng} & Y_{NW} & Y_{NN} \end{bmatrix} \begin{bmatrix} \Delta V_g \\ \Delta V_W \\ \Delta V_N \end{bmatrix} = Y_{close} \begin{bmatrix} \Delta V_g \\ \Delta V_W \\ \Delta V_N \end{bmatrix} \tag{8}$$

where ΔI_g and ΔI_W are the current variations at generator buses and FCWG bus respectively; ΔV_g, ΔV_W and ΔV_N are the voltage variations at generator buses, FCWG bus and other buses; Y_{close} is the admittance matrix of transmission network.

Eliminating the non-source buses, the network equation can be simplified as

Preprints (www.preprints.org) | NOT PEER-REVIEWED | Posted: 1 October 2020 doi:10.20944/preprints202010.0017.v1

$$\begin{bmatrix}\Delta I_g\\ \Delta I_W\end{bmatrix}=\begin{bmatrix}Y_{gg}-\frac{Y_{gN}Y_{Ng}}{Y_{NN}} & Y_{gW}-\frac{Y_{gN}Y_{NW}}{Y_{NN}}\\ Y_{Wg}-\frac{Y_{WN}Y_{Ng}}{Y_{NN}} & Y_{WW}-\frac{Y_{WN}Y_{NW}}{Y_{NN}}\end{bmatrix}\begin{bmatrix}\Delta V_g\\ \Delta V_W\end{bmatrix}=\begin{bmatrix}Y_{11} & Y_{12}\\ Y_{21} & Y_{22}\end{bmatrix}\begin{bmatrix}\Delta V_g\\ \Delta V_W\end{bmatrix} \tag{9}$$

From the second equation of (1), the second equation of (5) and (9), the relation between voltage variation and state variables are expressed as

$$\begin{bmatrix}\Delta V_g\\ \Delta V_W\end{bmatrix}=\begin{bmatrix}Y_{11}-D_g & Y_{12}\\ Y_{21} & Y_{22}\end{bmatrix}^{-1}\begin{bmatrix}C_g & C_W\end{bmatrix}\begin{bmatrix}\Delta X_g\\ \Delta X_W\end{bmatrix} \tag{10}$$

From the first equation of (1) and (5),

$$\frac{d}{dt}\begin{bmatrix}\Delta X_g\\ \Delta X_W\end{bmatrix}=\begin{bmatrix}A_g & 0\\ 0 & A_W\end{bmatrix}\begin{bmatrix}\Delta X_g\\ \Delta X_W\end{bmatrix}+\begin{bmatrix}B_g & 0\\ 0 & B_W\end{bmatrix}\begin{bmatrix}\Delta V_g\\ \Delta V_W\end{bmatrix} \tag{11}$$

From (10) and (11), the closed-loop state-space model of entire power system is derived as

$$\frac{d}{dt}\begin{bmatrix}\Delta X_g\\ \Delta X_W\end{bmatrix}=A_{closed}\begin{bmatrix}\Delta X_g\\ \Delta X_W\end{bmatrix} \tag{12}$$

where A_{closed} is characteristic matrix of the closed-loop power system considering the dynamics of FCWG and defined as

$$A_{closed}=\begin{bmatrix}A_g & 0\\ 0 & A_W\end{bmatrix}+\begin{bmatrix}B_g & 0\\ 0 & B_W\end{bmatrix}\begin{bmatrix}Y_{11}-D_g & Y_{12}\\ Y_{21} & Y_{22}\end{bmatrix}^{-1}\begin{bmatrix}C_g & C_W\end{bmatrix} \tag{13}$$

3.4. Impact of FCWG on Electromechanical Dynamics

By employing modal analysis on the open-loop and closed-loop characteristic matrices, the EOMs can be determined and compared. The EOMs are identified with the electromechanical loop correlation ratio (ELCR), which is defined as

$$ELCR=\frac{PF_{rotor}}{PF_{total}-PF_{rotor}} \tag{14}$$

where PF_{rotor} is the sum of participation factors (PFs) related to electromechanical oscillatory loop associated with state variables (i.e. the rotor speed ω and rotor angle δ) for all M SGs, and PF_{total} is the sum of PFs of all state variables.

For any oscillation mode, if ELCR is larger than 1, the oscillation mode is identified to be an EOM. Similarly, the FCWG dynamic correlation ratio (FDCR) can also be proposed to distinguish FCWG oscillation mode, which is defined as

$$FDCR=\frac{PF_{FCWG}}{PF_{total}-PF_{FCWG}} \tag{15}$$

where PF_{FCWG} is the sum of participation factors (PFs) related to all state variables of FCWG.

Since the MSC of FCWG is decoupled with the external power system, the most interactive part is the grid side converter (GSC) of FCWG, and it should be highlighted that the concept of FDCR can be extended to any other power source (e.g. voltage source converter (VSC)). Likewise, the methodology proposed in this paper can be applied to study impact on electromechanical dynamics from any kind of converter-based power sources (such as PV, energy storage system (ESS)).

Preprints (www.preprints.org) | NOT PEER-REVIEWED | Posted: 1 October 2020 doi:10.20944/preprints202010.0017.v1

In an EOM, two state variables (i.e. the rotor speed ω and rotor angle δ) related to the SG rotor are recognized as the main contributor to electromechanical oscillatory dynamics. For FCWG, there are usually two state variables taking part in the EOM most actively when strong interaction happens. Normally, a pair of state variables, which is closely related to a controller of FCWG (e.g. PLL controller, or DC voltage controller), might participate actively in electromechanical dynamics, and thus can be regarded as **quasi-electromechanical state variables**. Though these state variables are not from any physical rotational storage, their participation in an EOM will inevitably affect the electromechanical dynamic responses and might incur unintended consequences if not properly tackled.

If strong interaction between FCWG and the external power system, the quasi-electromechanical state variables may hold a considerable PF in an EOM, and thus ELCR in (14) may fall below 1. As a result, ELCR is not suitable for identifying EOMs. To fill in this gap, a quasi-ELCR (QELCR) is proposed to account for the two quasi-electromechanical state variables and defined as

$$QELCR = \frac{PF_{rotor} + PF_{QEWG}}{PF_{total} - PF_{rotor} - PF_{QEWG}} \tag{16}$$

where PF_{QEWG} is the sum of PFs of the two quasi-electromechanical state variables from FCWG.

For any oscillation mode with an FDCR larger than 1, it can be recognized as an FOM. By analyzing the ELCR and FDCR of the same EOM, it is possible to quantify the participation of FCWG. Normally, the dynamics of FCWG is not involved in the EOM, and thus it is straightforward to identify an EOM via ELCR. However, if FCWG dynamics is strongly coupled with the electromechanical dynamics, ELCR may be lower than 1. ELCR is no longer suitable for identifying the EOM and study the interaction between the electromechanical dynamics and FCWG dynamics. In such situation, two possible results may emerge: 1) the electromechanical dynamics may mingle with the FCWG dynamics, an EOM may be dominated by FCWG dynamics instead of the rotors of SGs, and is no longer a typical EOM, and thus can be identified as a quasi-EOM; and 2) a new quasi-EOM may be introduced (which may also be dominated by FCWG) and imposed on the rotor swing movements of SGs. To be more specific, a very interesting phenomenon may appear, in which, with the increase of FDCR and the decrease of ELCR, a typical EOM will gradually turn into a quasi-EOM, and at the same time, the most interactive FOM may have an ELCR larger than 1, and can be considered as a new quasi-EOM. Such transition from the electromechanical dynamics to the quasi electromechanical dynamics is rare but may occur if FCWG is strongly interacted.

With the criteria of ELCR and FDCR, it is capable to distinguish all the EOMs and FOMs, as presented in **Figure 5**. This mode identification criteria can be implemented to observe the unusual transition in electromechanical dynamics.

Preprints (www.preprints.org) | NOT PEER-REVIEWED | Posted: 1 October 2020 doi:10.20944/preprints202010.0017.v1

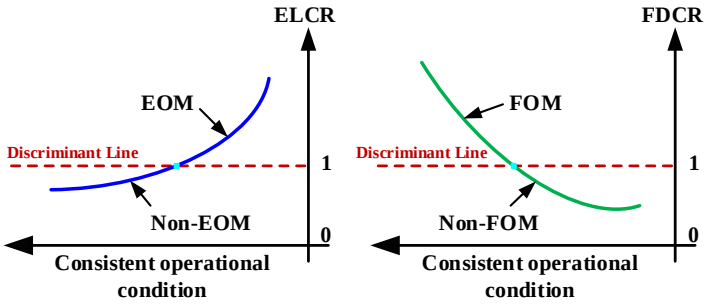

Figure 5. Criteria of EOM and FOM identification.

4. Case Study

4.1. Introduction of Test System

An FCWG-integrated modified two-area power system is set as a test system for investigation, as illustrated in **Figure 6**, in which the FCWG-base wind farm is connected at bus 12. Busbar 3 is the swing bus of the test system. To emulate the electromechanical dynamics, the simplified third-order model with a first order of the automatic voltage regulator (AVR) are adopted for each SG. No PSS is equipped. All the parameters of SGs parameters in [32] and parameters of FCWG in [12] are used, and detailed mathematical model can be found in [12, 32].

To cover the participation level, the FCWG is used to replace SG1 step by step. The **total active power output of FCWG and SG1 is 600MW and kept constant**. Other SGs and network and load parameters are the same throughout the following study.

The percentage of FCWG active power output **increases from 0% to 100% with a step length of 2%** (i.e. 12MW). Meanwhile, the active power from SG1 decreases from 100% to 0% with the same amount of power reduction.

The impact of FCWG on all the EOMs are analyzed through modal analysis. Mathematically, the dynamic interaction between FCWG and the external power system can be seen as modal coupling in which a major FOM interacts with the EOMs of the external power system. In other words, some state variables (at least two) of FCWG may participate in the EOMs, and state variables of rotor dynamics from SGs may also take part in the FOM that determined by these FCWG state variables.

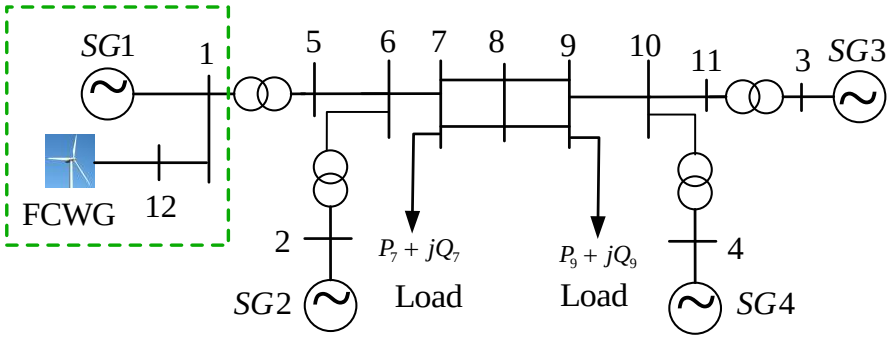

Figure 6. Configuration of two-area power system integrated with an FCWG wind farm.

The original EOMs of the two-area power system (i.e. the output of FCWG is Pew=0%) are identified and presented in **Table 1**.

Preprints (www.preprints.org) | NOT PEER-REVIEWED | Posted: 1 October 2020 doi:10.20944/preprints202010.0017.v1

Table 1. EOMs of Two-Area Power System (Pew=0.0%)

EOM No.	EOM1	EOM2	EOM3
Eigenvalue λ	-0.0660 + 3.3891i	-0.3201 + 5.7346i	-0.2824 + 5.9767i
Freq.(Hz)	0.5394	0.9127	0.9512
Damping Ratio	1.95%	5.57%	4.72%
ELCR	9.3952	23.7402	17.4803
FDCR	0	0	0
Major sources	SG3,SG4,SG1,SG2	SG2,SG1	SG4,SG3

The participation of power sources is also compared and demonstrated to clarify the relation between EOM and power sources, as shown in **Figure 7**. It is obvious that EOM1 is an inter-area oscillation mode that all SGs take part in, while EOM2 and EOM3 are two local oscillation modes that dominated by SG1,SG2 and SG3,SG4 respectively. Since FCWG is integrated in the left area, it is much likely that FCWG will participate in two EOMs (i.e. EOM1 and EOM2) and will not affect EOM3.

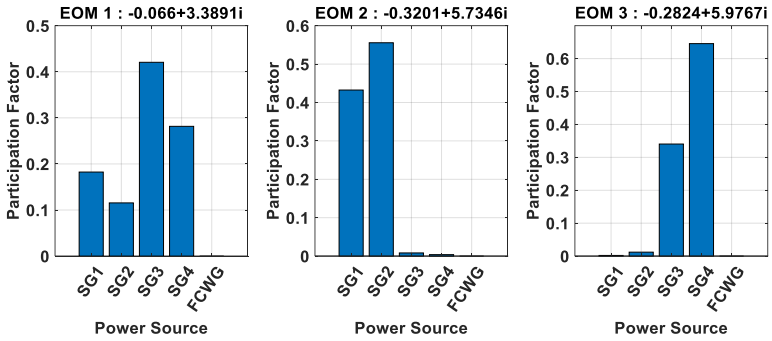

Figure 7. The participation of power sources in EOMs.

The participation of FCWG in EOM is not only affected by the power injection level, but also impacted by the parameters of FCWG controllers. The interaction between FCWG and the external power system are strongly related the relative locations of FOM and EOM. For a specific power system, EOMs normally do not vary too much and will stay at a relatively stable frequency. Meanwhile, the location of FOM are mainly determined by the controller parameters and operational conditions. The former is decisive as controller parameters can be designed with a bandwidth to accommodate signals of various oscillation frequencies. While the latter also affects the FOM location with different power flows, but such relation may not be decisive since it mainly attributes to the variation of voltage and current which are not strongly coupled in controller oscillation modes.

Table 2. Different Scenarios with respect to PLL-FOM under 50% FCWG Penetration level

Scenario No.	Parameters of PLL controller	PLL-FOM	EOM1	ELCR	FDCR
Scen. 1	Kipll=6, Kppll=1	-0.5243 +2.4481i	-0.1712 + .4044i	9.8518	0.0260
Scen. 2	Kipll=8, Kppll=1	-0.5057 +2.8071i	-0.1851 +3.4137i	7.2631	0.0601
Scen. 3	Kipll=10, Kppll=1	-0.4627 +3.1275i	-0.2233 +3.4200i	3.6326	0.1793
Scen. 4	Kipll=12, Kppll=1	**-0.4412 +3.5208i**	**-0.2397 +3.3226i**	**2.3364**	**0.2905**
Scen. 5	Kipll=14, Kppll=1	-0.4870 +3.7901i	-0.1889 +3.3257i	4.4731	0.1148
Scen. 6	Kipll=16, Kppll=1	-0.4986 +4.0331i	-0.1724 +3.3359i	6.1709	0.0632
Scen. 7	Kipll=100, Kppll=1	-0.4364 + 9.8689i	-0.1559 + 3.3686i	11.7832	0.0023

Preprints (www.preprints.org) | NOT PEER-REVIEWED | Posted: 1 October 2020 doi:10.20944/preprints202010.0017.v1

Table 3. Different Scenarios with respect to DC-FOM under 50% FCWG Penetration Level

Scenario No.	Parameters of DC voltage controller	DC-FOM	EOM1	ELCR	FDCR
Scen. 8	Kpi4=100, Kpp4=2	-0.0955 +1.8304i	-0.1614 + 3.3743i	11.5318	0.0061
Scen. 9	Kpi4=200, Kpp4=2	-0.1558 + 2.5672i	-0.1777 + 3.3826i	8.8525	0.0340
Scen. 10	Kpi4=300, Kpp4=2	**-0.1651 + 3.0997i**	**-0.2500 + 3.4155i**	**2.1014**	**0.3827**
Scen. 11	Kpi4=400, Kpp4=2	-0.3863 + 3.6959i	-0.1136 + 3.2919i	3.0269	0.1943
Scen. 12	Kpi4=500, Kpp4=2	-0.4665 + 4.0728i	-0.1201 + 3.3287i	5.9994	0.0612
Scen. 13	Kpi4=600, Kpp4=2	-0.5485 + 4.4338i	-0.1257 + 3.3402i	7.7275	0.0316
Scen. 14	Kpi4=2000, Kpp4=2	-1.8423 + 7.9388i	-0.1359 + 3.3565i	10.5869	0.0053

To give a thorough demonstration, two FOMs are selected to interact with the EOMs, i.e. the PLL-FOM which denotes the dynamics of PLL controller, and the DC-FOM which represents the dynamics of DC voltage controller. Therefore, different PI parameters are selected and denoted as different scenarios (under 50% FCWG penetration level), as presented in **Table 2** and **Table 3**. For Scenario 1~7, only the parameters of PLL controller change, and all other parameters of FCWG stay at the original. For Scenario 8~14, only the parameters of DC voltage controller vary, and all other parameters remain unchanged.

From the analysis above, it is noteworthy that in Scenario 4 and Scenario 10, FCWG has the most active participation in the electromechanical dynamics and hence possesses the best performances in improving EOM1. Comparing the FOMs in **Table 2** and **Table 3**, the oscillation frequencies of FOMs increase with the integral parameter of the controllers. When the oscillation frequencies of FOMs are close to the frequency of EOM1 (about 0.5Hz), the participation of FCWG becomes very active. When the FOMs move away, the participation of FCWG becomes less active.

4.2. Interaction between PLL-FOM and EOMs

Modal analyses are extensively implemented for every scenario considering 50 operational conditions (0%~100% penetration level of FCWG).

The interaction between PLL-FOM and EOM1, EOM2 are demonstrated in **Figure 8** and **Figure 9**, respectively. It is worth mentioning that the EOM3 is hardly influenced by the integration of FCWG, since it is another local EOM which is closely related to SG3 and SG4, and thus is not presented due to space limit.

Preprints (www.preprints.org) | NOT PEER-REVIEWED | Posted: 1 October 2020 doi:10.20944/preprints202010.0017.v1

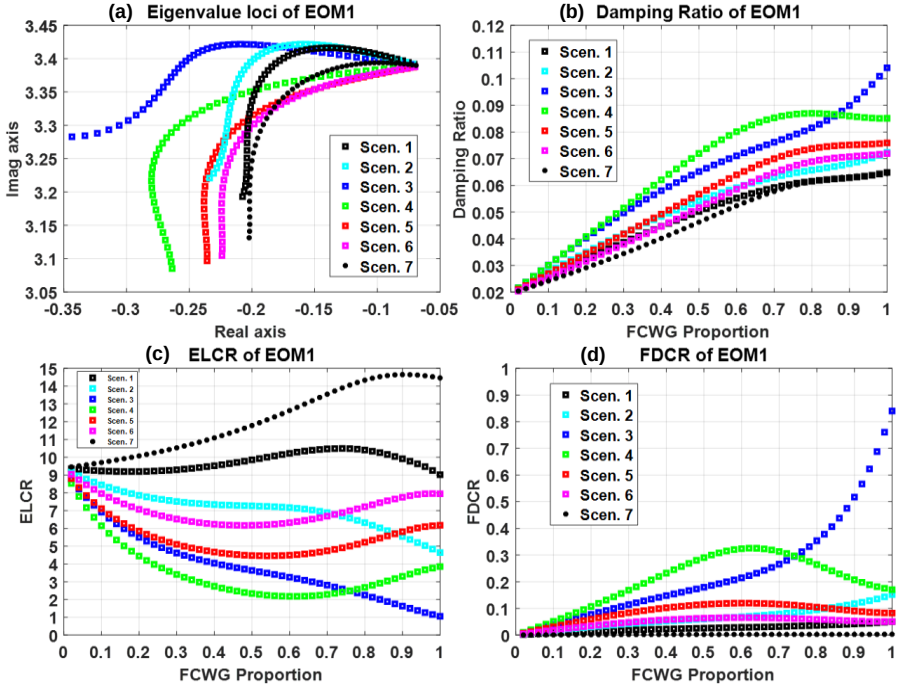

Figure 8. The interaction between PLL-FOM and EOM1 considering increasing FCWG proportion.

In Scenario 1~7, it is obvious that, the integration of FCWG is beneficial for EOM, as it is shown that in **Figure 8**(a), the eigenvalue of EOM1 turns to move towards the left in the complex plane, and **Figure 8**(b) further confirms that the damping ratio of EOM1 is enhanced. It is very interesting that, in **Figure 8**(c), the ELCR may increase or decrease under different scenarios. Particularly, for Scenario 3, the ELCR consistently decrease to almost 1, which indicates that EOM1 in gradually participated with other dynamics while the electromechanical dynamics becomes less and less active. Moreover, the FDCR in **Figure 8**(d) demonstrates that in most scenarios, the participation of FCWG in EOM1 stays at a very low ratio (Scenarios 1,2,5,6 and 7), which means the dynamic interaction of FCWG is weak, the damping enhancement are largely due to the power injection of FCWG. However, the FDCRs can increase significantly with Scenarios 3 and 4, and the damping ratio can also be raised a lot when FCWG participate actively. This indicates that dynamic interaction could be too strong to be ignored. It is surprising that such dynamic interaction is positive and may be utilized as a resort to enhance oscillation stability.

From **Figure 8**, it is concluded that, under some circumstance, strong interaction between FCWG and the external power system is possible. In this case, the integration of FCWG is conducive for EOM1, as depicted that the damping ratio of EOM is raised from 1.95% to over 10%, which is prominent from the perspective of low frequency oscillation suppression.

Preprints (www.preprints.org) | NOT PEER-REVIEWED | Posted: 1 October 2020 doi:10.20944/preprints202010.0017.v1

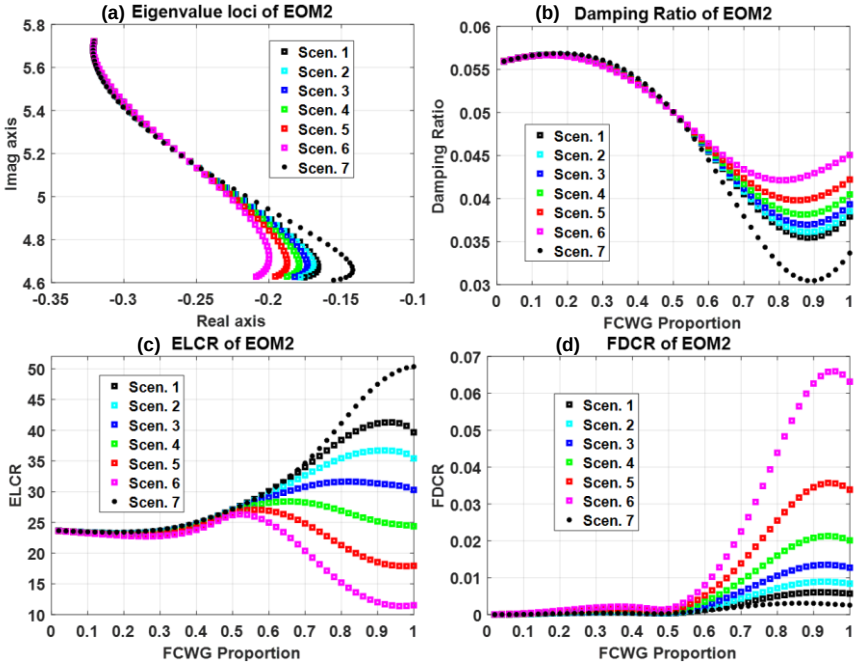

Figure 9. The interaction between PLL-FOM and EOM2 considering increasing FCWG proportion.

In Scenario 1~7, it is obvious that, the overall impact of FCWG integration is negative for EOM2, as it is shown that in **Figure 9**(a), the eigenvalue of EOM1 turns to move towards the right in the complex plane, and **Figure 9**(b) further confirms that the damping ratio of EOM1 is decreased.

The ELCRs in **Figure 9**(c) encounter some fluctuations under different scenarios, but stay above 10 all the time, which means EOM2 is always dominated by electromechanics dynamics. Whereas the FDCRs in **Figure 9**(d) are always less than 0.1, which indicates the participation of FCWG dynamics is very limited or even can be ignored. This finding validates that the damping deterioration of EOM2 is mainly attributed to the power injection of FCWG and power reduction of SG1.

From **Figure 9**, it is concluded that, the FCWG dynamics may not always hold considerable participation in the EOMs, and the power injection may become the main influence. The damping ratio of EOM2 is decreased from 5.57% to about 3%, which is a potential threat for this local EOM. Careful coordination for FCWG integration should be considered.

4.3. Interaction between DC-FOM and EOMs

From the analyses in Section 4.2, the parameters of PLL controller play an important role in the interaction between FCWG dynamics and electromechanical dynamics. With certain parameters in the PLL controller, FCWG can have a very active participation in electromechanical dynamics (e.g. Scenario 3&4).

To further validate the participation of FCWG, the parameters in DC voltage controller are also examined to investigate the interaction of DC-FOM and the EOMs. Accordingly, Scenario 8~14 are studied via modal analysis considering 50 operational conditions (which covers from 0% to 100% penetration level of FCWG with a 2% step). The results of interaction between DC-FOM and EOM1, EOM2 are depicted in **Figure 10** and **Figure 11**, respectively.

Preprints (www.preprints.org) | NOT PEER-REVIEWED | Posted: 1 October 2020 doi:10.20944/preprints202010.0017.v1

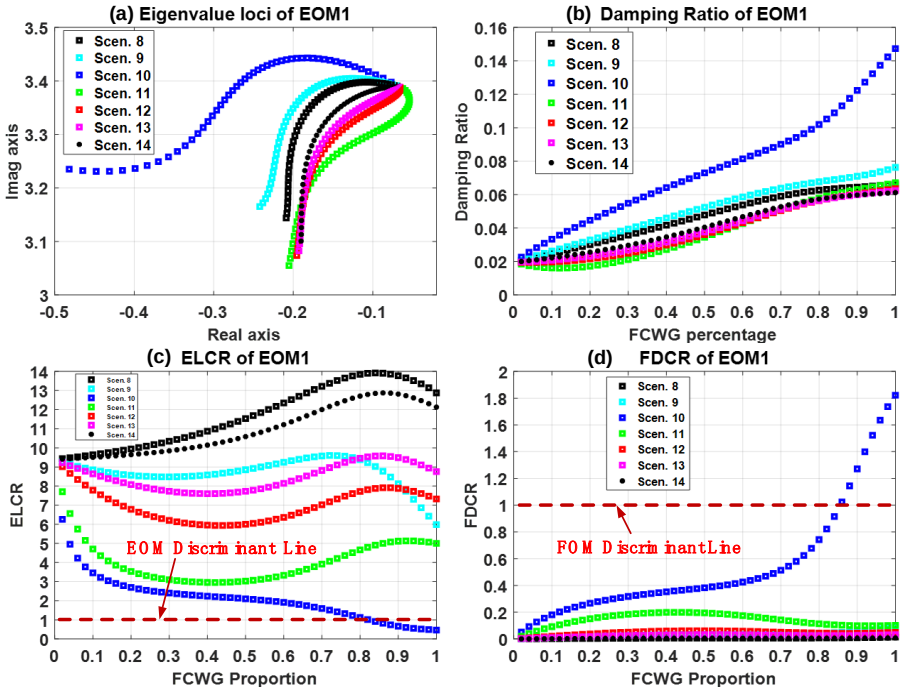

Figure 10. The interaction between DC-FOM and EOM1 considering increasing FCWG proportion.

In Scenario 8~14, the overall impact of FCWG integration is also beneficial for EOM1, as it is shown that in **Figure 10**(a), the eigenvalue of EOM1 turns to move towards the left in the complex plane. **Figure 10**(b) further confirms that the damping ratio of EOM1 is enhanced.

In **Figure 10**(c), the ELCR may also increase or decrease under different scenarios, which is similar as that of in **Figure 8**(c). However, when it comes to ELCRs and FDCRs, it should be highlighted that, for Scenario 10, the ELCR consistently decrease to below 1, which implies that EOM1 is no longer a typical EOM that determined by the electromechanical dynamics, and the participation of FCWG becomes the primary domination. As also verified in **Figure 10**(d), the FDCR in Scenario 10 can increase to above 1 at 86% penetration level, which also indicates this oscillation mode (i.e. previous identified to be EOM1) now becomes a quasi-EOM.

It is worth pointing that, although all scenarios can improve the damping ratio of EOM1, the contribution of damping enhancement due to FCWG integration are from two aspects: 1) power flow impact (which refers to the low participation of FCWG, such as Scenario 8~9, 12~14); and dynamic interaction impact (which could superpose dynamic impact on the electromechanical dynamics and even dominate the electromechanical oscillatory stability, such as Scenario 10).

From **Figure 10**, under some circumstance, strong interaction between FCWG and the external power system is possible. In Scenario 10, the integration of FCWG is conducive for EOM1, and the damping ratio of EOM1 can be raised from 1.95% to about 15%, which is quite impressive comparing with other scenarios (which can only reach about 8% damping ratio). This proves that dynamic interaction can be significantly and should not be ignored, and participation of FCWG matters a lot.

Preprints (www.preprints.org) | NOT PEER-REVIEWED | Posted: 1 October 2020 doi:10.20944/preprints202010.0017.v1

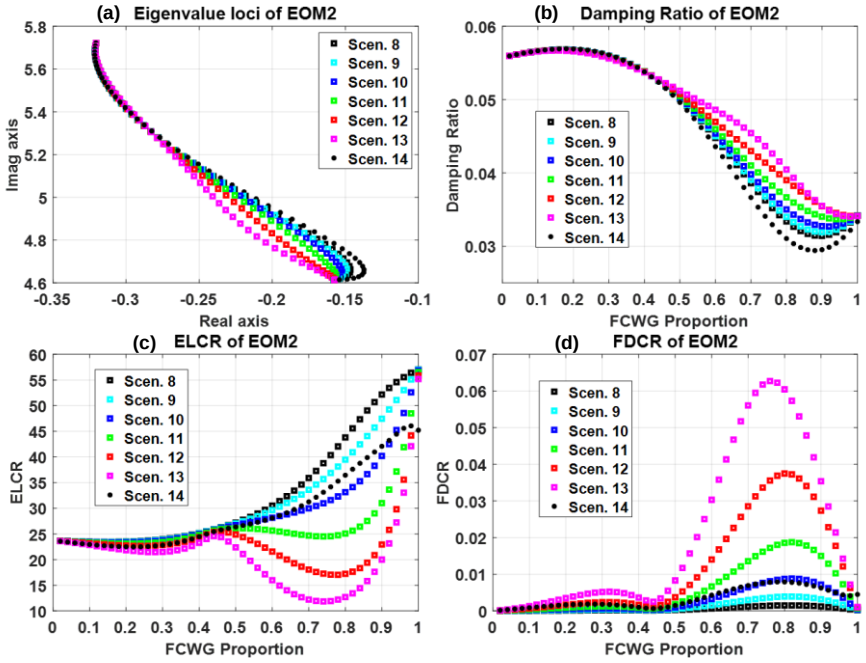

Figure 11. The interaction between DC-FOM and EOM2 considering increasing FCWG proportion.

The interactions between DC-FOM and EOM2 are shown in **Figure 11**. The damping ratio of EOM2 decreases in all scenarios, which indicates that the integration of FCWG is negative for EOM2. Such influence is mainly attributed to the power flow impact of FCWG, since the FDCRs are at a very low level (less than 0.1 as illustrated in **Figure 11**(d)). Though ELCRs in **Figure 11**(c) have encountered fluctuations, they are staying at a very high level (over 10), and thus the electromechanical dynamics of EOM2 is hardly affected by FCWG dynamics.

Table 4. EOMs of Two-Area Power System in Scenario 10(Pew=86%)

Mode No.	Eigenvalue λ	Freq. (Hz)	Damping Ratio	ELCR	FDCR
Open-loop power system					
Open EOM1	-0.1994 +3.2280i	0.5138	6.17%	17.4809	0
Open EOM2	-0.1677 +4.7219i	0.7515	3.55%	47.7340	0
Open EOM3	-0.2839 +5.9764i	0.9512	4.75%	17.9009	0
DC-FOM	-0.5333 +3.1585i	0.5027	16.65%	0	6.3587
Closed-loop power system					
Closed Mode 1	-0.2777 +3.0665i	0.4880	9.02%	**0.8911**	**0.8601**
Closed Mode 2	-0.3697 +3.2492i	0.5171	11.31%	**0.8194**	**1.0237**
Closed Mode 3	-0.1563 +4.6983i	0.7478	3.33%	36.6454	0.0084
Closed Mode 4	-0.2840 +5.9762i	0.9511	4.75%	17.8584	0

Particularly, take Scenario 10 as an example, major modes related to electromechanical dynamics in both open-loop power system and closed-loop power system model are demonstrated in **Table 4** (the FCWG proportion is 86%). Due to the strong interactions between FCWG dynamics and electromechanical dynamics, there are only two typical EOMs (i.e. EOM2 and EOM3) left in the closed-loop power system. The inter-area EOM 1 (i.e. 0.51Hz) is now dominated by FCWG with an

Preprints (www.preprints.org) | NOT PEER-REVIEWED | Posted: 1 October 2020 doi:10.20944/preprints202010.0017.v1

ELCR less than 1 and an FDCR larger than 1, and thus is a quasi-EOM. Local EOM2 is slightly affected while local EOM3 is hardly moved by comparing them with the closed-loop mode 3 and 4. The participation of power sources in four major oscillation modes are depicted in **Figure 12**. It is important to highlight that the active participation of not only dominates the inter-area mode (viz. Closed Mode 2) but also introduces a new quasi-EOM (i.e. Closed Mode 1), in which the electromechanical dynamics are involved.

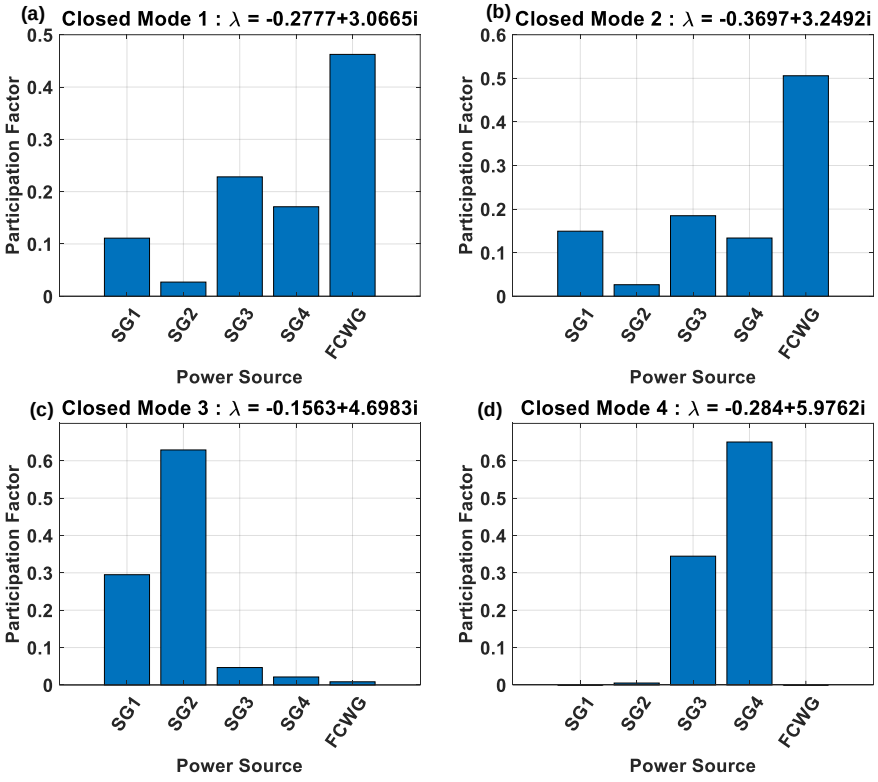

Figure 12. The participation of power sources in major oscillation modes of the closed-loop power system.

4.4. Time Domain Simulations for Verification of Frequency Domain Analysis

From the analysis above, it is noteworthy that in Scenario 4 and Scenario 10, FCWG has the most active participation.

To verify the above analyses, time domain simulations are also performed. The simulation condition is set: a 5% increase of mechanical output occurs at SG2 at 0.2s, and then drops the original value after 100ms. The FCWG penetration level is set to be 50% (i.e. 300MW), and all the parameters of the transmission network and generators are the same. To save space and maintain clarity, only Scenario 4, 7 and 10 are selected to implement the small disturbance simulations.

The angular speed, bus voltage and active power of SG3 are compared in **Figure 13**(a)~**Figure 13** (c). The reason why variables of SG3 are chosen for comparison is that, in time domain simulations, the variation of SG3 variables are formulated in the superposition of both local mode (EOM3) and inter-area mode (EOM1). The participation of FCWG affects both EOM1 and EOM2, whereas FCWG integration benefits EOM1 and deteriorates EOM2 at the same time, and these two EOMs will impose on the dynamic performances of SG1 and SG2 and may lead to misunderstanding. Therefore, by comparing variables of SG3 under different scenarios, the impact on EOM1 from the participation of FCWG can be clearly demonstrated.

Preprints (www.preprints.org) | NOT PEER-REVIEWED | Posted: 1 October 2020 doi:10.20944/preprints202010.0017.v1

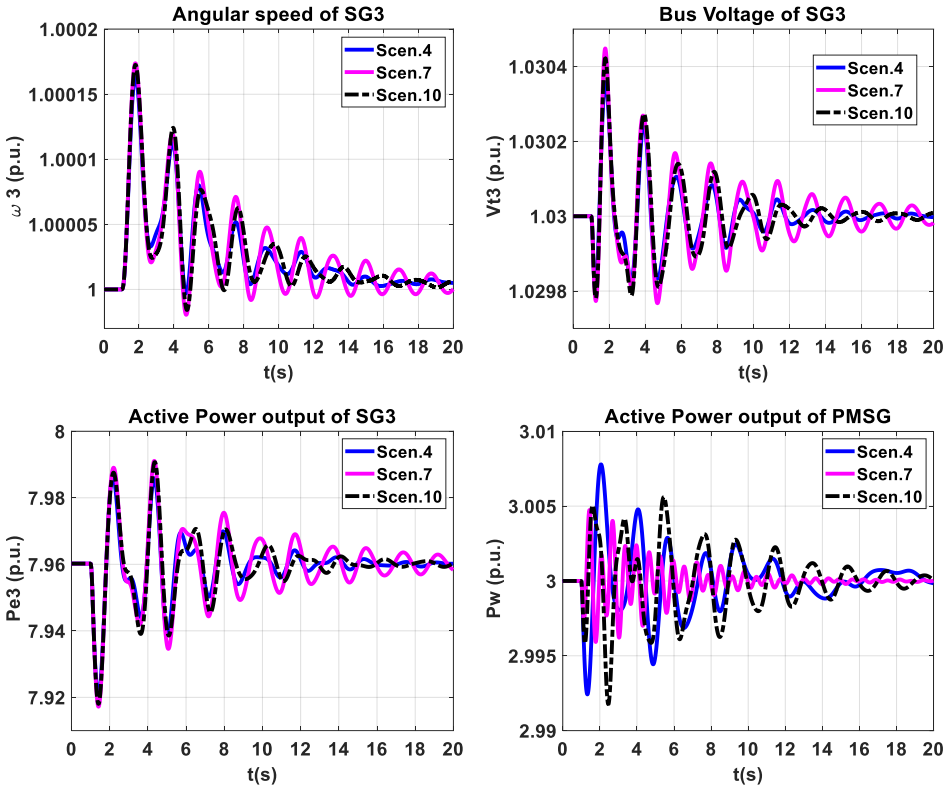

Figure 13. The dynamic responses of interaction between FCWG dynamics and electromechanical dynamics.

It is obvious that Scenario 4 and 10 have better dynamic performances than that of Scenario 7 in terms of electromechanical dynamics. This is because of the active participation of FCWG. It must also mention that the participation of FCWG in electromechanical dynamics may introduce negative effects on its own dynamics. For example, the active power of FCWG in Scenario 4 and 10 have worse dynamic performances than that of Scenario 7, as demonstrated in **Figure 13**(d). Therefore, the integration of FCWG may not only participate in the electromechanical dynamics and influence the oscillatory stability of the power system, the side effect on its own dynamic performances should also be carefully considered. Appropriate dynamic interaction coordination between FCWG dynamics and electromechanical dynamics is suggested when integrating FCWG into the power system.

4.5. Discussion on a Special Case: Replacement of SG with FCWG

The replacement of an SG with the FCWG will affect the electromechanical dynamics profoundly. On one hand, with the removal of an SG from the grid, the rotor swing dynamics of this SG is now excluded from the inter-area EOM. On the other hand, a local EOM related to this SG may also disappear (e.g., EOM 2 of the two-area benchmark system in this paper).

Normally, the FCWG is weakly participated in electromechanical dynamics and even can be ignored. However, if strong interaction between FCWG and the external power system occurs, two quasi-electromechanical state variables may act as that the electromechanical oscillatory loop associated state variables of the replaced SG, and hence introduces a new local quasi-EOM. Under such circumstances, the integration of FCWG becomes vital in determining power system oscillatory stability.

 doi:10.20944/preprints202010.0017.v1

5. Discussion

Based on all the analyses above, **some key findings with respect to the FCWG participation in electromechanical dynamics are summarized as bellow**

1) FCWG dynamics might interact with both inter-area EOM and local EOM;

2) The interaction can be either positive or negative, and may improve one EOM while deteriorate the other;

3) The degree of interaction is normally influenced by the penetration level of FCWG and the distance between the two affected modes. Strong interaction is more likely to occur at a high penetration level of FCWG, with the frequency of the FOM within the oscillation frequency range of EOM (i.e., 0.2Hz ~ 2.5Hz), especially when an FOM is close to an EOM;

4)When the strong interaction occurs,, the ELCR of the EOM may drop below 1, which indicates that this EOM is no longer electromechanical dynamics dominated, and accordingly, the FDCR of the EOM might increase above 1, which implies that this EOM has been determined by FCWG dynamics and thus transformed into a quasi-EOM;

5) Different FOMs with respect to different FCWG controllers may interact with the EOMs;

6) For the same FCWG controller, the integral parameter plays a key role in determining the oscillation frequency of the due FOM and thus affecting the participation of FCWG in the electromechanical dynamics;

7) In the cases of strong interaction, the integration of FCWG introduces a new quasi-EOM which relates to both system electromechanical dynamics and FCWG dynamics;

8) The participation of FCWG may not only affect the system electromechanical dynamics, but also influence the FCWG dynamics, and thus proper coordination of dynamic interaction is needed to avoid the negative effects.

6. Conclusion

Due to the decoupling nature of FCWG, its dynamics can be normally neglected when studying the system electromechanical dynamics, whereas the exceptional case is the strong interaction between wind and grid. In this paper, we have extensively investigated the participation of FCWG in electromechanical dynamics of the power system and how it transforms the characteristics of system EOM. By using the mode identification criteria, the participation of FCWG in system electromechanical dynamics is quantified. It is found that in most scenarios when the FOMs have an oscillation frequency far from that of EOMs, the participation of FCWG is quite limited, and the main impact of FCWG on EOM is via the power flow injection. However, when an FOM has a similar frequency to that of an EOM, the participation of FCWG may become significantly active, or even dominate the EOM. In this condition, a transition from the traditional electromechanical dynamics to quasi-electromechanical dynamics has been observed with the assistance of the proposed FDCR and QELCR.

Author Contributions: J.L. completed the methodology, analysis, simulation, validation, and wrote the paper. S.B. supervised the research throughout, coordinated the project, and revised & edited the paper. All authors have read and agreed to the published version of the manuscript.

Acknowledgments: The authors would like to acknowledge the support from National Natural Science Foundation of China for the Research Project (51807171), Guangdong Science and Technology Department for the Research Project (2019A1515011226), Hong Kong Research Grant Council for the Research Projects (25203917), (15200418) and (15219619), and Department of Electrical Engineering, The Hong Kong Polytechnic University for the Start-up Fund Research Project (1-ZE68).

Conflicts of Interest: The authors declare no conflict of interest.

References

1. Milano, F.; Dörfler, F.; Hug, G.; Hill, D. J.; Verbič, G. In *Foundations and challenges of low-inertia systems*, 2018 Power Systems Computation Conference (PSCC), 2018; 2018; pp 1-25.
2. Sun, J.; Li, M.; Zhang, Z.; Xu, T.; He, J.; Wang, H.; Li, G., Renewable energy transmission by HVDC across the continent: system challenges and opportunities. *CSEE J. Power Energy Syst* **2017,** 3, (4), 353-364.
3. Hatziargyriou, N.; Milanović, J.; Rahmann, C.; Ajjarapu, V.; Cañizares, C.; Erlich, I.; Hill, D.; Hiskens, I.; Kamwa, I.; Pal, B., Stability definitions and characterization of dynamic behavior in systems with high penetration of power electronic interfaced technologies. *IEEE PES Technical Report PES-TR77* **2020,** 42.
4. Li, Y.; Gu, Y.; Zhu, Y.; Ferre, A. J.; Xiang, X.; Green, T. C., Impedance Circuit Model of Grid-Forming Inverter: Visualizing Control Algorithms as Circuit Elements. *IEEE Trans. Power Electron.* **2020**, 1-1.
5. Gu, Y.; Li, Y.; Zhu, Y.; Green, T., Impedance-Based Whole-System Modeling for a Composite Grid via Embedding of Frame Dynamics. *IEEE Trans. Power Syst.* **2020**, 1-1.
6. Gautam, D.; Goel, L.; Ayyanar, R.; Vittal, V.; Harbour, T., Control Strategy to Mitigate the Impact of Reduced Inertia Due to Doubly Fed Induction Generators on Large Power Systems. *IEEE Trans. Power Syst.* **2011,** 26, (1), 214-224.
7. Hedayati-Mehdiabadi, M.; Zhang, J.; Hedman, K. W., Wind Power Dispatch Margin for Flexible Energy and Reserve Scheduling With Increased Wind Generation. *IEEE Trans. Sustainable Energy* **2015,** 6, (4), 1543-1552.
8. Garmroodi, M.; Hill, D. J.; Verbic, G.; Ma, J., Impact of Tie-Line Power on Inter-Area Modes With Increased Penetration of Wind Power. *IEEE Trans. Power Syst.* **2016,** 31, (4), 3051-3059.
9. Bialasiewicz, J. T.; Muljadi, E. In *The wind farm aggregation impact on power quality*, IECON 2006-32nd Annual Conference on IEEE Industrial Electronics, 2006; 2006; pp 4195-4200.
10. Knüppel, T.; Nielsen, J. N.; Jensen, K. H.; Dixon, A.; Østergaard, J., Power oscillation damping capabilities of wind power plant with full converter wind turbines considering its distributed and modular characteristics. *IET Renewable Power Gener.* **2013,** 7, (5), 431-442.
11. Knüppel, T.; Nielsen, J. N.; Jensen, K. H.; Dixon, A.; Ostergaard, J., Small-signal stability of wind power system with full-load converter interfaced wind turbines. *IET Renewable Power Gener.* **2012,** 6, (2), 79-91.
12. Luo, J.; Bu, S.; Zhu, J.; Chung, C. Y., Modal Shift Evaluation and Optimization for Resonance Mechanism Investigation and Mitigation of Power Systems Integrated With FCWG. *IEEE Trans. Power Syst.* **2020,** 35, (5), 4046-4055.
13. Du, W.; Chen, X.; Wang, H., PLL-Induced Modal Resonance of Grid-Connected PMSGs With the Power System Electromechanical Oscillation Modes. *IEEE Trans. Sustainable Energy* **2017,** 8, (4), 1581-1591.
14. Ying, J.; Yuan, X.; Hu, J.; He, W., Impact of Inertia Control of DFIG-Based WT on Electromechanical Oscillation Damping of SG. *IEEE Trans. Power Syst.* **2018,** 33, (3), 3450-3459.
15. Sun, L.; Liu, K.; Hu, J.; Hou, Y., Analysis and Mitigation of Electromechanical Oscillations for DFIG Wind Turbines Involved in Fast Frequency Response. *IEEE Trans. Power Syst.* **2019,** 34, (6), 4547-4556.
16. Singh, M.; Allen, A. J.; Muljadi, E.; Gevorgian, V.; Zhang, Y.; Santoso, S., Interarea Oscillation Damping Controls for Wind Power Plants. *IEEE Trans. Sustainable Energy* **2015,** 6, (3), 967-975.
17. Silva-Saravia, H.; Pulgar-Painemal, H. In *Effect of Wind Farm Spatial Correlation on Oscillation Damping in the WECC System*, 2019 North American Power Symposium (NAPS), 13-15 Oct. 2019, 2019; 2019; pp 1-6.
18. Mokhtari, M.; Aminifar, F., Toward Wide-Area Oscillation Control Through Doubly-Fed Induction Generator Wind Farms. *IEEE Trans. Power Syst.* **2014,** 29, (6), 2985-2992.

19. Liao, K.; He, Z.; Xu, Y.; Chen, G.; Dong, Z. Y.; Wong, K. P., A Sliding Mode Based Damping Control of DFIG for Interarea Power Oscillations. *IEEE Trans. Sustainable Energy* **2017,** 8, (1), 258-267.
20. Boubzizi, S.; Abid, H.; Chaabane, M., Comparative study of three types of controllers for DFIG in wind energy conversion system. *Protection and Control of Modern Power Systems* **2018,** 3, (1), 21.
21. Gurung, N.; Bhattarai, R.; Kamalasadan, S., Optimal Oscillation Damping Controller Design for Large-Scale Wind Integrated Power Grid. *IEEE Trans. Ind. Appl.* **2020,** 56, (4), 4225-4235.
22. Morató, J.; Knüppel, T.; Østergaard, J., Residue-Based Evaluation of the Use of Wind Power Plants With Full Converter Wind Turbines for Power Oscillation Damping Control. *IEEE Trans. Sustainable Energy* **2014,** 5, (1), 82-89.
23. Fan, L.; Yin, H.; Miao, Z., On Active/Reactive Power Modulation of DFIG-Based Wind Generation for Interarea Oscillation Damping. *IEEE Trans. Energy Convers.* **2011,** 26, (2), 513-521.
24. Elhaji, E. M.; Hatziadoniu, C. J. In *Damping tie line oscillation using permanent magnet wind generators in the Libyan power system*, 2014 North American Power Symposium (NAPS), 7-9 Sept. 2014, 2014; 2014; pp 1-6.
25. Bu, S.; Du, W.; Wang, H., Model validation of DFIGs for power system oscillation stability analysis. *IET Renewable Power Gener.* **2017,** 11, (6), 858-866.
26. Bu, S. Q.; Zhang, X.; Zhu, J. B.; Liu, X., Comparison analysis on damping mechanisms of power systems with induction generator based wind power generation. *Int. J. Electr. Power Energy Syst.* **2018,** 97, 250-261.
27. Xia, S. W.; Bu, S. Q.; Zhang, X.; Xu, Y.; Zhou, B.; Zhu, J. B., Model reduction strategy of doubly-fed induction generator-based wind farms for power system small-signal rotor angle stability analysis. *Appl. Energy* **2018,** 222, 608-620.
28. Jafarian, M.; Ranjbar, A. M., Interaction of the dynamics of doubly fed wind generators with power system electromechanical oscillations. *IET Renewable Power Gener.* **2013,** 7, (2), 89-97.
29. Ge, Y.; Cai, H.; Cao, J.; Wang, H. F. In *Impact of large scale wind power penetration on power system oscillations based on electric torque analysis*, International Conference on Sustainable Power Generation and Supply (SUPERGEN 2012), 8-9 Sept. 2012, 2012; 2012; pp 1-7.
30. Luo, J.; Bu, S.; Teng, F., An optimal modal coordination strategy based on modal superposition theory to mitigate low frequency oscillation in FCWG penetrated power systems. *Int. J. Electr. Power Energy Syst.* **2020,** 120, 105975.
31. Wilches-Bernal, F.; Chow, J. H.; Sanchez-Gasca, J. J. In *Impact of wind generation power electronic interface on power system inter-area oscillations*, 2016 IEEE Power and Energy Society General Meeting (PESGM), 17-21 July 2016, 2016; 2016; pp 1-5.
32. Kundur, P.; Balu, N. J.; Lauby, M. G., *Power system stability and control*. McGraw-hill New York: 1994; Vol. 7.